Light Metals 2012 *Edited by: Carlos E. Suarez*
TMS (The Minerals, Metals & Materials Society), 2012

OBSERVATION OF STRUCTURE EVOLUTION DURING ANNEALING OF 7XXX SERIES AL DEFORMED AT HIGH TEMPERATURE

Cory G. Parker and David P. Field
School of Mechanical and Materials Engineering, Washington State University, Pullman, WA 99164-2920

Keywords: 7050 aluminum alloy, geometrically necessary dislocation density, recrystallization

Abstract

Deformation of polycrystalline materials results in a heterogeneous distribution of dislocation structures that are dependent upon the local character of the microstructure. 7xxx series aluminum alloys are particularly complex because of the wide range of particles and solute atoms that are in the material. High temperature deformation results in a microstructure that may be essentially free from dislocation structures at one position but have relatively high dislocation content at another position. Electron backscatter diffraction was used to quantify and map the dislocation density tensor at various positions through the metal. Subsequent annealing resulted in the development of recrystallization nuclei that were also observed by EBSD and related to the measured dislocation structure.

Introduction

Industrial processing of 7xxx series aluminum alloys generally involves hot deformation of the material at some point. During this process, the ingot structure is completely broken down and a more refined structure develops that is replete with dislocations and other crystalline defects. The character of the microstructure in this condition provides a plate with more homogeneous properties than existed in the cast ingot. The nature of the defects determines the downstream behavior of the material, whether the kinetics of structural evolution during further processing, or the mechanical properties of the material in service. In spite of the attempt to homogenize properties, the nature of the defect structure, particularly for products with somewhat limited deformation, is necessarily heterogeneous [1-5]. This heterogeneity is a function of the homogenized ingot structure as well as the processing parameters and conditions. Quantification of such structure is problematic, but can be estimated by x-ray or neutron diffraction.

Over the past decade, measurement of part of this deformation structure has become possible using electron backscatter diffraction (EBSD) based techniques [6-10]. This enables the point to point determination of the defect structure and can aid in understanding the heterogeneity that develops. The geometrically necessary dislocation density tensor is related to lattice curvature as determined by a systematic measurement of crystallite orientation over a regular grid of points in three-dimensions. The actual dislocation density cannot be measured, but a component of this structure can be estimated by EBSD measurements.

Experimental Details

A 125 mm (5 inch) thick AA 7050 plate was hot rolled by standard industrial processes and before solutionizing and aging was quenched in water in an attempt to capture the hot-rolled structure. Five samples in total were cut from the center section of the plate as indicated in Figure 1. Four samples of various sizes were cut with the plane of analysis herein referred to as the plan view section (the plane normal to the plate normal direction). In addition, one long transverse sample was cut from the middle center of the plate (planes normal to the plate transverse direction). The long transverse sample represents the top portion of the plate with a finished polished face of 6.3 cm, the 4 samples from the plan view represent faces 1.3, 3.2, 5.2, and 7 cm from the bottom of the plate. All 5 samples underwent grinding on SiC abrasive sandpaper as grits of 120, 240, 400, and 1200. All samples were then cleaned in a ultrasonic cleaner before being air dried. Samples were moved in a "figure 8" pattern on the polishing wheel while it was stationary using 1 micron diamond paste for approximately 10 minutes for each sample. Blue lube was used as the diamond extender to ensure proper lubrication of the wheel while the sample was polished. The cleaning process using the ultrasonic cleaner was then repeated to ensure that all particles from the previous step had been removed from the surface of the sample. The sample was then polished on a polishing wheel using 0.05 micron alumina powder solution and cleaned in the same manner as before. The 4 plan view samples were then put in an automatic vibratory polish machine with 0.02 micron colloidal silica for approximately 75 minutes and cleaned once more. The LT sample was polished using the same machine, however, it was polished manually for approximately 75 minutes due to its large size and cleaned in the normal procedure.

All samples were examined using standard (EBSD) practices at a tilt angle of 70°, an accelerating voltage of 20 keV, and a step size of 2 microns over a regular hexagonal grid. The 4 plan view samples were all scanned between 7 and 10 times at various positions using a 250x magnification. The LT sample was scanned primarily at 100x magnification at intervals of between 0.3 and 0.5 cm between the centers of each scan. The first 2 mm of the LT sample from the surface exhibited pitting due to the manual nature of the vibratory polish and as such 4 scans were taken at 250x magnification in this pitted area in order to get a clear picture of dislocation density in the area. Overall 16 scans were done through the thickness of the plate on the LT sample. Data was then imported into TSL OIM Analysis 5.1 and cleaned by removing all points with a Confidence Index value less than 0.2 and using Grain CI Standardization to ensure that no erroneous data were included in the calculations. No orientations were artificially added to the data set. In-house software [10,11] was used to calculate geometrically necessary dislocation density. This software utilizes the dislocation density tensor in order to calculate GNDs across the scans. The dislocation density tensor as originally defined by Nye [6] can be written as:

$$\alpha_{ij} = e_{ikl}\left(\varepsilon^{e}_{jl,k} + g_{jl,k}\right) \quad (1)$$

where α_{ij} represents the dislocation density tensor, e_{ikl} represents the permutation tensor, $\varepsilon_{jl,k}$ represents the elastic strain gradient, and $g_{jl,k}$ represents the lattice curvature measured by EBSD. Using this relation, assumptions must be made that eliminate the

elastic strain gradient term. In addition, since these measurements are made from 2-D sections, the character and curvature of the direction normal to the plane represented by the EBSD scans is ignored. Another relation between the dislocation density tensor and density of dislocation types is given by:

$$\alpha_{ij} = \sum_k \left(b_i^k z_j^k\right) \rho^k \qquad (2)$$

where the dislocation density tensor is still represented by α_{ij}, ρ^k represents the density of dislocations of the k^{th} type of dislocation represented by the Burger's vector, b, and line direction, z. And so, using equations 1 and 2, the term ρ can be solved for, giving the density of GNDs at any given point given the lattice curvature present as measured by EBSD. This process was automated by the in-house software. Densities are represented in the software by a repurposed Image Quality map with usual minimum and maximum values between 0 and $20{,}000 \times 10^{11}$ m^{-1}. However, calculations were done regarding the geometry of the system and the maximum dislocation density was estimated to be about 2000×10^{11} m^{-2} and a subsequent assumption was made in order to eliminate grain boundaries, which were defined as being found as any point to point misorientation of over 5°, from the data by making the minimum dislocation density taken into account 0.01×10^{11} m^{-1}, even though the minimum measureable density using a step size of 2 μm is closer to 20×10^{11} m^{-2}. This assumption worked out well as over 90% of all data in a single scan fit in the range between 0.01×10^{11} and 2000×10^{11} m^{-1}.

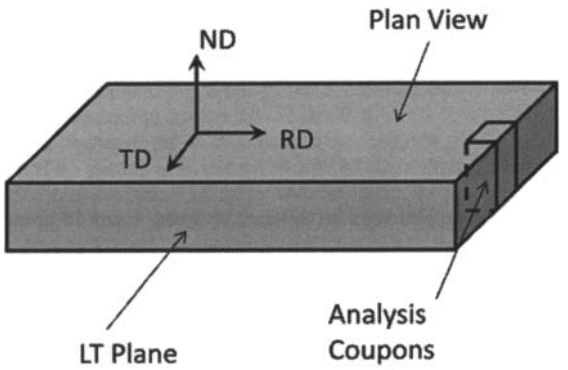

Figure 1 – Schematic of rolled plate and region indicated from where analysis coupons were manufactured.

Results and Discussion

Orientation images were constructed from each location analyzed through the plate thickness. Figure 2 shows a representative map from a section near the mid-plane of the plate. A map of the corresponding geometrically necessary dislocation density as calculated from the EBSD data is shown in Figure 3. Regions near grain boundaries of greater than 5 degrees were ignored in the calculation and any points bordering bad data were also ignored in the calculation. Dislocation densities as determined from plan view sections are shown in Figure 4 for each of the four locations measured. These results are the average of 5 scans on each section plane and do not reflect the observed heterogeneity in the structure. It is evident from Figure 4 that a slightly higher GND density is present near the surface of the specimens as compared with the plate interior regions. This is likely a reflection of the varying amounts of strain in the specimen and presumably tracks in a manner consistent with the total dislocation density.

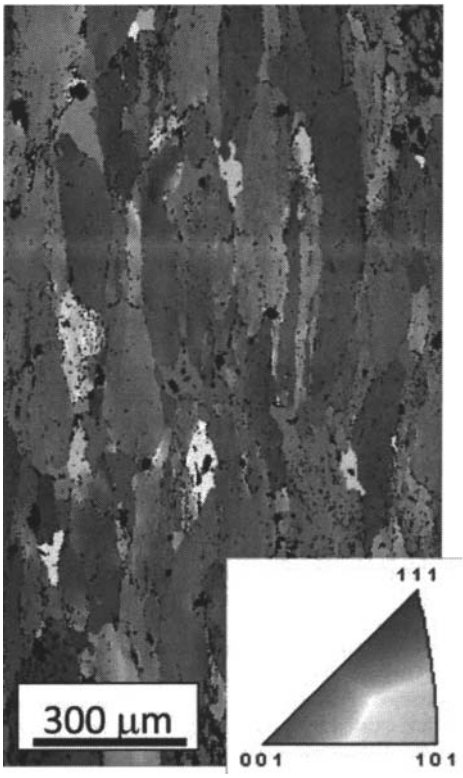

Figure 2 – Orientation image from a plan view region near the mid-plane of the plate.

The most useful measure of the dislocation density at varying points through the thickness of the plate proved to be the scans from the LT sample since the dislocation density could be obtained in more positions than was performed for the plan view sections. Dislocation density at the surface was calculated to be 400×10^{11} m^{-2} while density near the mid-thickness (t/2) was measured to be 250×10^{11} m^{-2} with a steady decline occurring between these two points. Figure 5 contains the average values from each plate position analyzed in a manner similar to that shown for the plan view data presented in Figure 4. Large scan areas were used to ensure that a great number of grains were included at each position to strengthen the statistics. These large scan areas also revealed the inhomogeneity in the density of the GNDs measured. When looking at density maps from the software it is clear that in larger grains there is a clear correlation between proximity to grain boundaries and density of GND. This correlation makes it obvious that dislocations begin to form during the rolling procedure and move through the lattice before encountering the nearest grain boundary. Because it requires a large expenditure of energy to move across such a large misorientation spread the dislocation stops and the process repeats, growing the density near grain boundaries more as compared to in the middle of the grain. This is the main reason getting a large number of grains in each scan of an area is

important, as one is more likely to find high densities near boundaries as compared to in the middle of large grains.

Because of the need to use a large number of grains in order to construct strong statistics it became necessary in some locations, especially when scanning the plan view sections, to do several scans and merge them together to provide an average of the measured dislocations densities. These averages are what are represented in the data shown. Data shown from the LT sample are also averages of the GND density in each scan. Because in this study GND density is linked to higher lattice energy the average density displays an idea of the average relative lattice energy at different locations through the thickness of the plate as compared to other positions. This usage of an average does not display the maximum density measured, but instead allows different planes through the thickness of the plate to be selected as most likely to contain high enough densities to provide the energy necessary for recrystallization to occur during the solutionizing and aging processes.

Figure 3 –Image showing the distribution of GND near the mid-plane of the plate as determine from the EBSD data shown in Figure 2.

The maximum density values, which represent the truest measure of where recrystallization will occur, do not track in the same way that average density values do. Instead, the maximum values fluctuate between $19{,}000x10^{11}$ m^{-2} and $20{,}000x10^{11}$ m^{-2} until close to the t/4 positions when grain size begins to increase by an extremely noticeable amount. This increase in grain size causes all maximum density values from t/4 to t/2 to drop to between $18{,}000x10^{11}$ m^{-2} and $19{,}000x10^{11}$ m^{-2}. This large drop in maximum measured density can be attributed to the same effect that creates the large densities to begin with. Because grains have not be affected by the rolling process as much and have stayed relatively large dislocations are more free to move throughout the lattice in these large grains. In effect there is more surface area per grain in these larger grains at which the dislocations can stuck up, allowing for densities that are lower to form, while still maintaining a heterogeneous structure in line with the trend observed through the thickness of the plate.

It is also important to discuss the statistical reliability of these measurements and results. The average values of density range from $400x10^{11}$ m^{-2} to $250x10^{11}$ m^{-2} while the standard deviation on these values is $200x10^{11}$ m^{-2} and $160x10^{11}$ m^{-2} respectively. The large standard deviation does not arise largely because of an error or uncertainty in the measurement, but because of the inhomogeneous nature of the structure. Standard deviations are based on the overall population where each pixel is counted as a measurement. Pixels near grain boundaries are generally observed to have high values of GND density, while those away from the boundary may have lower values. Each value is added to the total population and the mean and standard deviation is determined using the standard procedure. In addition, because measurements had to were made in two dimensions Equations 1 and 2 become less reliable, but far easier to work with because they require fewer inputs. This creates data that displays little certainty in precision, but the data itself is not wrong in the trend it provides. Because the error is present in all scans and positions through the thickness of the plate the average values used in this study create a lower bound at each position. This lower bound outlines the general trend that occurs while moving through the thickness of the rolled plate. It should also be mentioned that the step size of the EBSD scan impacts the accuracy of the data collected by introducing scan resolution issues as well as by impacting the dislocation density able to be measured. According to Field et al. [12] as step size of EBSD scans increases the measured dislocation content decreases. At a step size of 2 microns the expected GND calculation resolution should be between $80x10^{11}$ m^{-2} and $400x10^{11}$ m^{-2} depending on angular resolution. A resolution of about $400x10^{11}$ is to be expected in the present study as the angular resolution is on the order of 0.5 degrees.

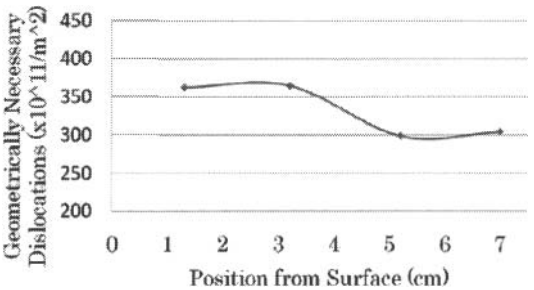

Figure 4 – GND density as a function of position through the plate thickness as measured from plan view sections (planes normal to the plate ND).

The general trend for total GND density through the thickness found in both the plan view and LT samples is that content is higher closer to the surface and decreases moving towards t/2. While this general trend was present in both plan view and LT samples the actual measured values differed somewhat, with the LT sample showing GND density decreasing much more quickly than the measurements of the plan view samples. Two separate trends presented themselves during data analysis. The first is that while moving from surface to t/2 grain size increased greatly, most notably starting at the t/4 position.

The second is that despite the immediate quenching following the hot rolling process recrystallization was present in every scan done on the LT sample with a somewhat parabolic trend that starts high at the surface, decreases to a plateau near t/4 and rises again near t/2. Recrystallized grains have been defined as grains with a Grain Orientation Spread of less than 1°. These characteristics most likely all come from the hot rolling technique used. Because of the way strain is applied to the plate during rolling grains will be deformed much greater than at t/2, which accounts for the large difference in grain size and the decrease in overall GND content from surface to t/2. The presence of recrystallization at all points in the sample is harder to accept due to the immediate quench that occurred after hot rolling. However, due to the temperature at which the hot rolling occurs, and the high level of strain present throughout the plate, new crystals could have possibly formed during the time the plate took to quench.

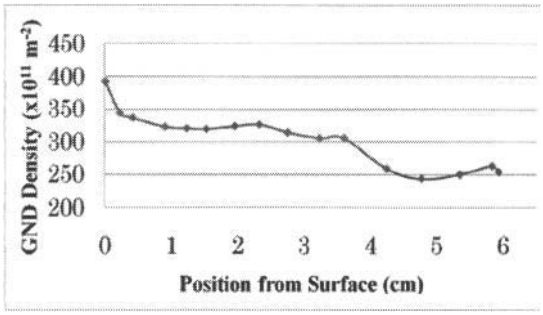

Figure 5 – GND Density as a function of position through the plate thickness

Conclusions

A partial measure of the dislocation content in a deformed polycrystalline material can be obtained by means of EBSD measurements. This geometrically necessary dislocation density has a strong local heterogeneity but over a large region tends to be a reasonable estimate of stored energy in the material. Estimates of GND density from plan view sections and from LT sections of a rolled plate of 7xxx series aluminum showed average results that were similar to each other. The GND density was highest near the rolled surface of the plate and dropped off steeply to a plateau. At about t/4 the GND density as measured by this technique tended to drop off again to another plateau to the mid-point of the plate (t/2). It is anticipated that the kinetics of recrystallization will be at least partially dependent upon the stored energy of the plate as measured by EBSD estimates of the GND density.

Acknowledgements

This work was partially supported by the National Science Foundation's Research Experience for Undergraduates program under grant number DMR-0755055.

References

1. Flemings MC, Nereo GE 1968 *Trans. AIME*, **242,** 50
2. Beaudoin AJ, Cassada WA, Proc. TMS Spring Meeting, (1998).
3. Robson JD, Prangnell PB 2001 *Acta Mater*, **49**, 599
4. Robson, JD *Mat. Sci. Eng. A*, **382**, 112
5. Gore BE, Harnish S, Padilla H, Robinson BJ, Beaudoin AJ, Dantzig JA, Robertson IM, Weiland H, 2003 *Hot Deformation of Aluminum Alloys III* TMS, Pittsburgh, PA, pp. 255-262.
6. Nye JF 1953 *Acta Metall*, **1** 153
7. Ashby MF 1970 *Phil. Mag*, **21** 399
8. Kröner E 1981 Continuum Theory of Defects. Physics of Defects, North-Holland, Amsterdam
9. El-Dasher BS, Adams BL, Rollett AD 2003 *Scripta Mater*, **48** 141
10. Field DP, Trivedi PB, Wright SI, Kumar M 2005 *Ultramicroscopy*, **103** 33
11. Merriman CC, Field DP, Trivedi P 2008 *Matls. Sci. Eng. A*, **494** 28
12. Field DP, Merriman CC, Allain-Bonasso N, Wagner F 2011 *Mod. Sim. Matls. Sci. Eng. in Press.*